

CONF-770401--30

APPLICATION OF AN ADVANCED SHIELDING ANALYSIS SYSTEM
TO GAS-COOLED FAST REACTOR DESIGNS*

D. E. Bartine and L. R. Williams

Oak Ridge National Laboratory

NOTICE
This report was prepared as an account of work sponsored by the United States Government. Neither the United States nor the United States Energy Research and Development Administration, nor any of their employees, nor any of their contractors, subcontractors, or their employees, makes any warranty, express or implied, or assumes any legal liability or responsibility for the accuracy, completeness, or usefulness of any information, apparatus, product, or process disclosed, or represents that its use would not infringe privately owned rights.

By acceptance of this article, the publisher or recipient acknowledges the U.S. Government's right to retain a nonexclusive, royalty-free license in and to any copyright covering the article.

*Research sponsored by the Energy Research and Development Administration under contract with the Union Carbide Corporation.

MASTER

UNLIMITED

86

APPLICATION OF AN ADVANCED SHIELDING ANALYSIS SYSTEM
TO GAS-COOLED FAST REACTOR DESIGNS

D. F. Bartine and L. R. Williams
Oak Ridge National Laboratory
Oak Ridge, Tennessee, USA

ABSTRACT

In its shielding program for General Atomic's Gas-Cooled Fast Reactor (GCFR), Oak Ridge National Laboratory has developed an advanced shielding analysis system that incorporates the latest analysis techniques for converging to a shield design compatible with other design parameters. Basically the system consists in applying the various techniques in a logical sequence to a given design, thereby generating a large body of data to serve as an information base for subsequent redesigns by General Atomic. The first step is a discrete ordinates radiation transport calculation for a two-dimensional model of the reactor system. The resulting neutron and gamma-ray fluxes are then converted to isoplots of the responses of concern, and these are used to locate regions in the system at which those responses are higher than allowed by predetermined constraints. Next, adjoint calculations are performed for the regions of concern, and the resulting adjoint fluxes, together with the forward fluxes, are used in channel-theory calculations to determine the physical paths followed by the particles traveling from the core to those regions. In addition, the adjoint and forward fluxes are used in sensitivity calculations to determine the importance of the cross sections used in the transport calculations as functions of the shield materials and particles energies. Finally, the sensitivity results are utilized in the form of linear perturbation theory to predict the effect of changes in the shield composition and position on the various responses. This system is being applied to successive reference models for the GCFR and on the basis of the data obtained thus far the thickness of the radial shield has been significantly reduced and the lower shield region has undergone extensive redesign. The design-analysis-redesign iterations will continue until they converge upon an acceptable demonstration configuration.

INTRODUCTION

During the past decade Oak Ridge National Laboratory's arsenal of calculational tools for performing reactor shielding analyses has increased to the extent that one of the primary responsibilities of the shield evaluators is to develop a logical sequence for applying the various techniques in a given situation. In addition, they must determine which, if any, of the techniques, or the nuclear data used in them, require experimental confirmation with respect to the particular application being made. At ORNL,

"integral" testing of the methods or data is done with experiments performed at the Tower Shielding Facility (TSF).

In its shielding program for General Atomic's Gas-Cooled Fast Reactor (GCFR), ORNL has developed an advanced shielding analysis system that incorporates these latest analysis techniques for converging to a shield design compatible with other design parameters, such as those dictated by cooling and structural requirements, material compatibility, etc. The large body of data generated from the analysis then serves as an information base for a subsequent redesign by General Atomic (GA). The redesign itself is subjected to a similar analysis, which yields another data base, and the iteration continues until a satisfactory design is arrived at.

Table 1. Available Methods and Codes for Shielding Analysis

Transport Calculations:
Discrete ordinates (S_n)
DOT (two-dimensional)
ANISN (one-dimensional)
Monte Carlo
MORSE (three-dimensional)
Coupled
DOT-DOMINO-MORSE
Channel Theory Analysis: FANG
Sensitivity Analysis:
SWANLAKE (one-dimensional)
VIP (two-dimensional)
Uncertainty Analysis: FORSS

The ORNL methods and codes currently available for shielding analyses are listed in Table 1. They include codes with which radiation transport throughout the reactor-shield system can be calculated in one, two, or three dimensions, both in the forward mode and in the adjoint mode; a technique for coupling two- and three-dimensional transport calculations at a common boundary; a channel-theory analysis technique which allows a determination of the channels in space through which the important radiation particles travel; sensitivity analysis methods for determining the sensitivity of the one- or two-dimensional transport calculations to the cross sections used in them; and an uncertainty analysis system which allows a determination of

the uncertainty on the calculated response due to uncertainties associated with the nuclear data used in the calculations.

In a typical application of these techniques to the GCFR, the first step is a discrete ordinates radiation transport calculation for a two-dimensional model of the reactor-shield system. The resulting neutron and gamma-ray fluxes are then converted to isoplots of the responses of concern (radiation damage, heating, etc.), and these are used to locate regions in the system at which those responses are higher than allowed by predetermined constraints. Next, adjoint calculations are performed for the regions of concern, and the resulting adjoint fluxes, together with the forward fluxes, are used in channel-theory calculations to determine the physical paths followed by the particles traveling from the core to those regions. In addition, the adjoint and forward fluxes are used in sensitivity calculations to determine the importance of the cross sections used in the transport calculations as functions of the shield materials and particle energies. Finally, the sensitivity results are utilized in the form of linear perturbation theory to predict the effect of changes in the shield composition and position on the various responses.

In some cases (although none are discussed in this paper), transport calculations for specific regions of the system are calculated in three

dimensions and the results are coupled to the two-dimensional calculations of adjacent or surrounding regions. The three-dimensional calculations are usually limited to regions that have complicated geometries difficult to describe in two dimensions. However, usually two-dimensional calculations are also performed for these regions so that by comparison with the three-dimensional calculations the adequacy of two-dimensional representations of three-dimensional problems can be determined. Also, on occasion the two-dimensional descriptions are such as to represent a "worst-case" situation for the region in question and thereby to set upper limits on the radiation transport through the region. And, of course, prototypic or semiprototypic experiments are sometimes performed to determine geometric effects and to investigate techniques for modeling complicated geometries. Another paper at this Conference reports the results of one such experiment performed in the GCFR shielding program.¹

To date, FORSS uncertainty analyses have not been carried out in the GCFR program, but the plan is to perform them later. FORSS couples cross-section uncertainty estimates in the Evaluated Nuclear Data Files (ENDF) with the cross-section sensitivities determined for the calculated response for a particular reactor-shield system and arrives at an uncertainty on the response due to uncertainties in the nuclear data used to calculate it. FORSS also has the capability for using the results from relevant experiments as a basis for "adjusting" the nuclear data used in the calculations within the bounds of their uncertainties.

CALCULATIONS FOR INITIAL REFERENCE DESIGN

The shield analysis system described above was applied to the initial GCFR reference calculational model shown in Fig. 1. While some studies have concentrated on determining the neutron fluxes in the vicinity of the grid plate shown above the reactor core, the area of investigation presented in this paper is concerned with the neutrons that leave the reactor core in the downward direction, heading toward the lower deck. These neutrons may reach the prestressed concrete reactor vessel (PCRV) by streaming around the lower end of the radial outer shield, by penetrating through the wraparound shield, or by streaming into the lower axial helium channel. In these first calculations the purpose was to determine the fluxes of the neutrons that followed each of these paths to the liner and the resulting radiation heating produced at each location. The quantities were then to be compared with the maximum allowable values of each that were recommended.

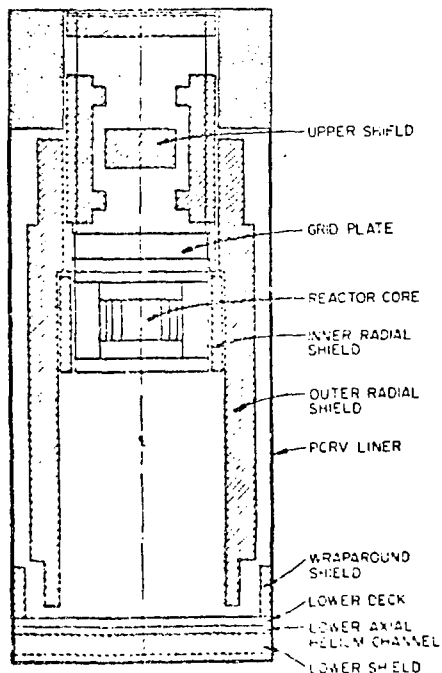


Fig. 1. Two-Dimensional GCFR Calculational Model.

The calculations were performed in two-dimensional geometry with the

discrete ordinates code DOT. A preliminary calculation used a P_1 Legendre expansion of a 50-group neutron cross-section set and had a homogeneous representation of the inner and outer radial shields (50% graphite and 50% type 304 stainless steel). This was followed by a calculation in which these shields were represented as laminated sections of graphite and stainless steel, and a P_3 expansion of a cross-section set including 51 neutron groups and 25 gamma-ray groups was employed. A comparison of the two calculations showed that the second model resulted in a 30% increase in the high-energy flux transmitted to the liner and a concomitant decrease in the thermal-neutron flux.

The results from the calculation based on the laminated shield model are shown in the first part of Table 2 (Initial Model results). For this model the maximum values above the wraparound region occur just above the wraparound shield. The recommended restraints have been adapted from HTRC (High-Temperature Gas-Cooled Reactor) criteria and should not be viewed as being firm.

Table 2. Comparison of Calculated Results for Two-Dimensional Models of GCFR

Parameter and Position	Calculational Results			
	Recommended Constraint	Lower Axial He Channel	Wraparound Region	Maximum Above Wraparound Region
Initial Model				
$\phi(E>1 \text{ MeV}), * \text{PCRVR Liner}$	2 + 9	2.4 + 7	7.1 + 7	5.3 + 7
$\phi(E<2.38 \text{ eV}), * \text{PCRVR Liner}$	1 + 9	3.7 + 10	3.3 + 10	7.8 + 10
Heating in PCRVR (mW/cm^3)	1 + 0	0.7 + 0	1.0 + 0	1.8 + 0
Heating in Tendon Lubricant (rads)	1 - 1	5.5 + 0	7.7 + 0	1.2 + 1
Revised Model				
$\phi(E>1 \text{ MeV}), * \text{PCRVR Liner}$	2 + 9	9.9 + 7	1.8 + 8	5.0 + 8
$\phi(E<2.38 \text{ eV}), * \text{PCRVR Liner}$	1 + 9	4.6 + 10	8.5 + 9	1.6 + 9
Heating in PCRVR (mW/cm^3)	1 + 0	0.9 + 0	0.3 + 0	0.3 + 0
Heating in Tendon Lubricant (rads)	1 - 1	7.1 + 0	4.3 + 0	2.4 + 0
New Revised Model				
$\phi(E>1 \text{ MeV}), * \text{PCRVR Liner}$	2 + 9	1.5 + 7	2.5 + 8	5.0 + 8
$\phi(E<2.38 \text{ eV}), * \text{PCRVR Liner}$	1 + 9	3.7 + 10	8.2 + 9	26.4 + 9
Heating in PCRVR (mW/cm^3)	1 + 0	0.7 + 0	1.7 + 0	1.2 + 0
Heating in Tendon Lubricant (rads)	1 + 0	0.8 + 0	9.6 + 0	8.1 + 0

*Neutrons $\text{cm}^{-2} \text{sec}^{-1}$.

The initial model calculations revealed that the high-energy neutron flux along the PCRVR liner is not a problem, but that the thermal-neutron flux exceeds the recommended restraint at all locations. Neither does gamma-ray heating in the liner appear to be a problem, although it does exceed the constraint above the wraparound region. The heating in the lubricant for the tendons compressing the PCRVR is excessive, however, especially above the wraparound region. On the other hand, the recommended restraint is given in rads in grease whereas the calculated values are rads in concrete. (The data required to calculate rads in grease were not available.)

Isoplots of the thermal-neutron fluxes calculated for the initial model are shown in Fig. 2. The isoflux contours show the streaming up the outside of the outer radial shield and indicate that the maximum contour extends above the wraparound shield, its value being 7×10^{10} neutrons $\text{cm}^2 \cdot \text{sec}^{-1}$. It appeared that with the addition of B₄C as a thermal poison and proper shield redesign, a reduction in the radial dimension of the radial dimension of the reactor cavity might be possible.

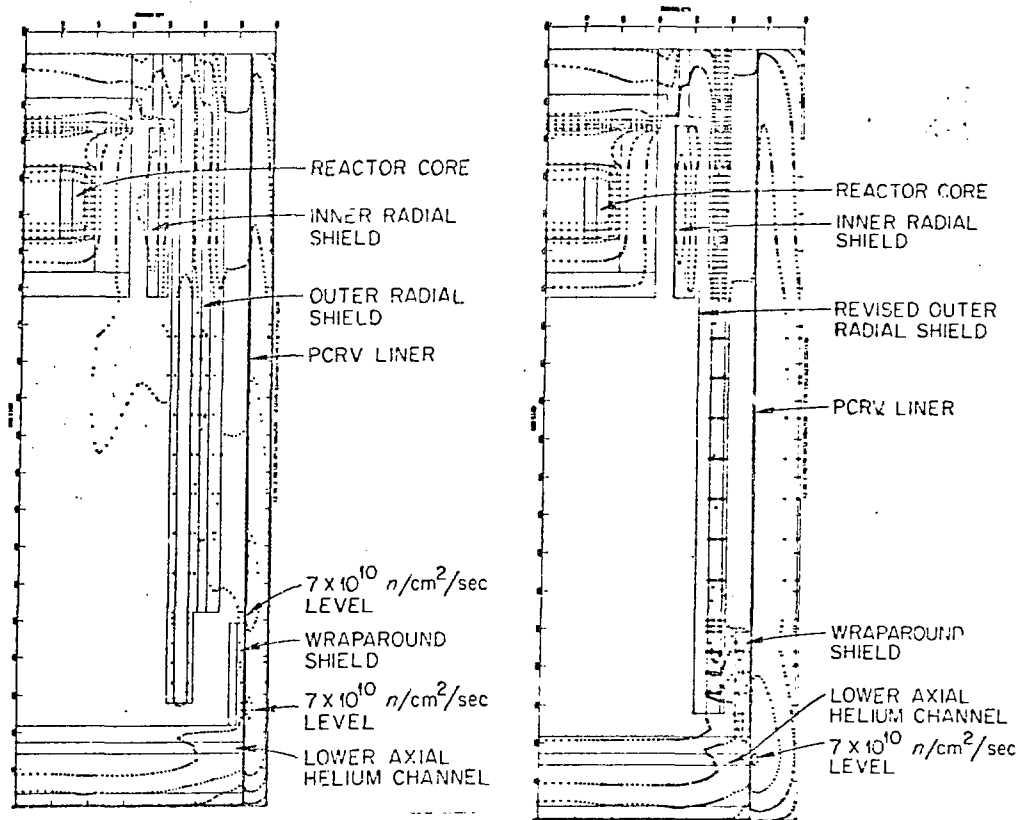


Fig. 2. Isoplots of Thermal-Neutron Fluxes ($E < 2.38$ eV) for Initial (Left) and Revised (Right) Calculational Models.

CALCULATIONS FOR REVISED REFERENCE DESIGN

A study of potential revised radial shield designs was carried out by General Atomic, and as a result the outer radial shield thickness was reduced by 1 ft. The revised outer shield consisted of an 18-cm-thick graphite layer followed by an 18-cm-thick graphite-B₄C mixture (about 19% B₄C by weight) and a 5-cm-thick stainless steel 304 region. A corresponding reduction in the radius of the PCRV was also made.

Calculations for the revised design shown in the second part of Table 2 reveal that the high-energy neutron flux is still maintained well below the constraint, the maximum fluxes on the PCRV liner occurring this time at a location just below the inner shield. The gamma-ray heating in the liner also remains below the constraint. However, the thermal-neutron flux at the liner is still too high, as is the heating in the tendon lubricant. An isoplot of the thermal-neutron flux included in Fig. 2 (above, right) indicates a high flux level at the lower axial helium channel and wrap-around position but a reduced level above the wrap-around shield.

A series of adjoint calculations for the revised design were then initiated, including calculations for the thermal-neutron flux levels in the PCRV liner at the lower axial helium channel and wrap-around shield, for PCRV gamma-ray heating at the lower axial helium channel, and for the gamma-ray dose in the tendon lubricant at the lower axial helium channel and

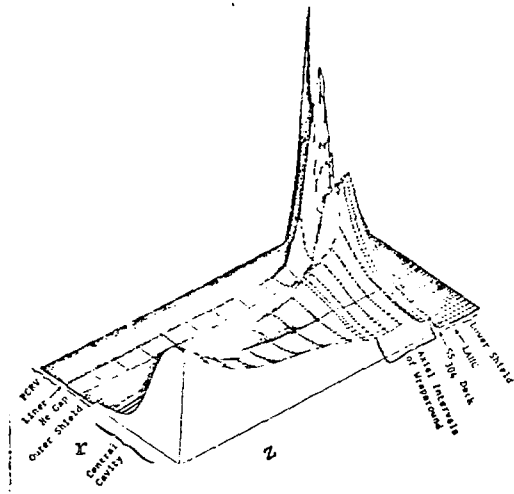


Fig. 3. Plot Showing Pathways of Contributors Producing Gamma-Ray Dose in Tendon Lubricant at Wrap-around Shield Level (Revised Model).

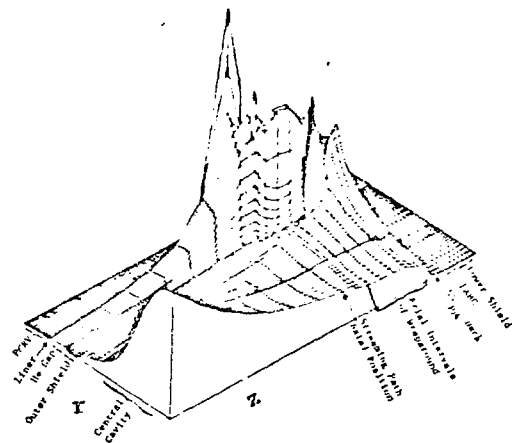


Fig. 4. Plot Showing Pathways of Contributors Producing Thermal-Neutron Fluxes in PCRV Liner Above Wrap-around Shield (Revised Model).

wraparound shield. The resulting adjoint fluxes were then used, together with the forward fluxes, in the FANG channel-theory code to produce three-dimensional plots of the contributor fluxes, where a "contributor" is a particle that contributes to the response of interest. Thus, the plots depict the passage of contributing particles from the reactor core to the location where the response has been determined.

A plot showing the pathways taken by the contributors that produce the gamma-ray dose in the tendon lubricant at the wraparound shield level is shown in Fig. 3, where the corner in the lower center of the figure is located just below the reactor core on the axis of the assembly. Thus the upper part of the figure represents the lower section of the assembly, which contains the lower shield, the lower axial helium channel, etc. (compare with Figs. 1 and 2). Since the gamma rays reaching the location of interest are gamma rays produced by the capture of neutrons, the contributors plotted in Fig. 3 are both neutrons and gamma rays, the neutrons being followed to their point of capture and the gamma rays being followed thereafter. The plot shows a primary streaming path around the outer shield, the first peak occurring in the helium gap just below the shield. The second peak occurs in the PCRV liner, where thermal neutrons are captured in the iron. The highest peak occurs in the PCRV at the tendon position itself, where thermal-neutron capture in the concrete contributes the major fraction of the dose.

Interpretation of Fig. 3 is aided by the plot shown in Fig. 4. Here the contributors plotted are those responsible for the thermal-neutron fluxes in the liner just above the wraparound shield. Again the plot shows a primary streaming path under the outer radial shield and back up the helium gap outside the shield. Also, the major peak again occurs in the PCRV, where the contributing neutrons are thermalized. Thus this plot primarily indicates the paths of high-energy neutrons to regions where they are thermalized and then transported to the location of interest in the liner.

Table 3. Sensitivity and Origin of Thermal-Neutron Flux at PCRV Liner Above Wraparound Shield

SENSITIVITY	% OF RESPONSE DUE TO THERMAL NEUTRON PRODUCTION IN REGION		REGION
-7.28-1	8.225+0		PCRV LINER
-1.85-2	1.089-1		LOWER SHIELD
-7.02-2	1.772-2		GRAPHITE (OUTER SHIELD)
-3.47-2	8.042-6		C+B ₄ C (OUTER SHIELD)
-1.89	1.309-3		C+B ₄ C (WRAPAROUND)
-4.66-1	8.216-1		SS ₃₀₄ DECK
-5.35-1	9.543+0		SS ₃₀₄ (WRAPAROUND)
-3.74-3	1.003-4		SS ₃₀₄ (OUTER SHIELD)
<u>3.24-2</u>	<u>77.773</u>		PCRV
-3.977	96.496		

Table 4. Sensitivity and Origin of Gamma-Ray Dose in Tendon Lubricant at Wraparound Shield Level

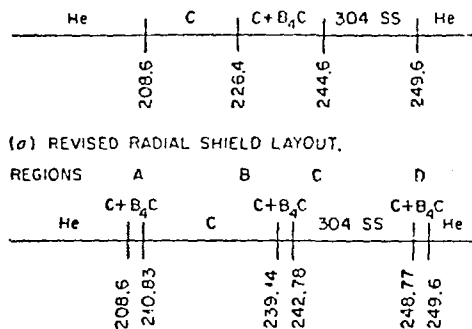
SENSITIVITY			PERCENT OF RESPONSE DUE TO GAMMA PRODUCTION IN ZONE	DESCRIPTION
NEUTRON	GAMMA	TOTAL		
-5.41-2	-1.22-2	-6.63-2	5.416	LOWERSHIELD
-7.79-1	-5.65-2	-8.36-1	5.106	SS DECK
-2.93-1	-2.47-4	-2.93-1	0.0	He COOLANT
-3.29-2	-2.61-3	-3.55-2	8.52-2	OUTER SHIELD GRAPHITE
-3.37-2	-2.63-3	-3.63-2	3.71-5	OUTER SHIELD C+B ₄ C
-3.17-3	-5.21-3	-8.38-3	2.23-2	OUTER SHIELD SS ₃₀₄
-1.446	-1.89-2	-1.465	2.74-4	B ₄ C+C WRAPAROUND
-4.97-1	-2.13-1	-7.10-1	3.48-1	SS ₃₀₄ WRAPAROUND
-6.35-2	-8.14-2	-1.92-1	9.888	PCRV LINER
-4.21-1	-1.176	-1.598	<u>76.14</u>	PCRV
-3.628	-1.569	-5.245	97.01	

Additional information on the thermal neutrons and gamma rays in the vicinity of the PCRV liner was obtained from sensitivity studies performed with the VIP code, which also required the forward and adjoint fluxes as input. Table 3 presents the sensitivities calculated for the thermal-neutron flux in the PCRV liner at the wraparound level, where the sensitivity is the predicted change in the flux per percent increase in the macroscopic neutron cross section for the spatial region indicated. The table also shows where most of the thermal neutrons contributing to the response are born (that is, where the high-energy neutrons are thermalized). These results show that the thermal-neutron flux at the liner is primarily sensitive to the neutron transport through the wraparound shield, especially through that portion of the shield consisting of C and B₄C, and that it is also sensitive to the neutron transport through the liner itself. The table also confirms that most of the thermal neutrons contributing to the flux are born in the PCRV.

The sensitivity of the gamma-ray dose at the tendon position at the wraparound level to both the neutron macroscopic cross section and the gamma-ray macroscopic cross section of the various spatial regions is given in Table 4, which also shows where the gamma rays contributing to the response are born. These results indicate that the gamma-ray dose is also primarily sensitive to neutron transport through the wraparound shield, but is also fairly sensitive to the SS-304 deck. Of the gamma rays at the tendon position, 76% are produced in the PCRV, most by thermal-neutron capture but some by epithermal capture.

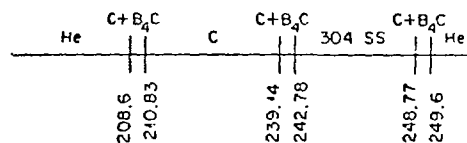
All the above results indicate that the high thermal-neutron fluxes and gamma-ray heating responses at the PCRV liner are attributable to high-energy neutrons being transported to the region and being thermalized and captured there. From this it can be inferred that redesigning the shields between the core and the liner to reduce the neutron flux levels would alleviate the problem.

Since the adjoint and forward calculations were already available for the revised shield design, it was relatively easy to examine possible alterations to the design by using two-dimensional linear perturbation theory. The initial shield layout and the perturbations to it are shown in Fig. 5, and predicted changes in various responses produced by the perturbations



(a) REVISED RADIAL SHIELD LAYOUT.

REGIONS



(b) PERTURBATIONS TO REVISED RADIAL SHIELD.

Fig. 5. Revised Radial Shield with Perturbations.

Table 5. Predicted Percent Change in Responses Due to Perturbations in the Revised Shield Design

RESPONSE	PREDICTED PERCENT CHANGE				TOTAL
	REGION A	REGION B	REGION C	REGION D	
R1	-1.947+1	5.928-1	1.587-1	-1.693-1	-1.869+1
R2	-6.223+0	5.223-1	5.063-1	-7.359-1	-5.901+0
R3	-6.525+1	2.119+1	6.667+0	-2.679+2	-3.033+2
R4	-1.384+1	4.270-1	2.120-1	-2.578-1	-1.346+1
R5	-3.685+2	5.143-1	3.847-1	-8.432-3	-3.684+2
R6	-3.730+1	5.685-1	1.846-1	-2.029-1	-3.335+1

R1 - E < 2.38 eV FLUX AT LINER AT THE LAHC LEVEL.
 R2 - E < 2.38 eV FLUX AT LINER AT THE WRAPAROUND REGION.
 R3 - E < 2.38 eV FLUX AT LINER AT THE STREAMING PATH POSITION.
 R4 - GAMMA DOSE AT TENDON AT THE LAHC LEVEL.
 R5 - GAMMA DOSE AT TENDON AT THE WRAPAROUND REGION.
 R6 - GAMMA HEATING IN THE PCRV AT THE LAHC LEVEL.

given in Table 5. The perturbations to the shield are as follows:

- Region A: $C+B_4C$ replaces C in the first 2.23 cm of the shield.
- Region B: C replaces $C+B_4C$ in the first 12.74 cm of original $C+B_4C$ region.
- Region C: SS-304 replaces $C+B_4C$ in the last 1.82 cm of original $C+B_4C$ region.
- Region D: $C+B_4C$ replaces SS-304 in the last 0.83 cm of the shield.

The results of this study indicate that the thermal-neutron flux and gamma-ray dose and heating are all strongly affected by the boronation of the inner edge of the outer shield (Region A). Other changes were not too significant except for the thermal-neutron flux along the streaming path, which was dominated by the effects of boronating the outer edge of the outer radial shield (Region D). It should be kept in mind, however, that these results were obtained from linear perturbation theory and therefore only indicate the relative magnitudes of large effects; they do not show actual results from a calculation of a revised design.

CALCULATIONS FOR NEW REVISED REFERENCE DESIGN

Subsequent to the calculations described above, a new revised design was provided by GA which represented a more realistic mockup of the lower shielding. The major changes included the removal of the outer borated graphite section of the outer radial shield at its lower end and the substitution of type 316 stainless steel for type 304 stainless steel. In addition, design changes were made in the stainless steel deck, the wrap-around shield, the lower shield, and several other components. The results of DOT two-dimensional calculations for this new revised reference design are included in Table 2. They show considerably increased values for the thermal-neutron flux and gamma-ray heating in the tendon lubricant above the wraparound shield region, both large factors above the criteria. Thus additional redesign will be required.

SUMMARY

This paper has presented the shielding analyses of GA-supplied calculational models of both an unboronated radial shield in a large-radius cavity and a boronated radial shield in a reduced-radius cavity, as well as preliminary results for a third more realistic model. Isoflux and isoheating plots were obtained for the models, and maximum response positions were located. Sensitivity analyses were performed to determine the importance of the cross sections used in the calculations for the revised model as a function of energy and material, and channel theory plots were obtained to determine the physical path taken by the particles in going from the core to the position of interest. The sensitivity analysis results were then utilized in the form of linear perturbation theory to predict the result of changing the shield composition and position.

All the data have been submitted to GA to serve as an information base for subsequent designs. Thus far the investigation indicates the feasibility of a reduced radial cavity coupled with the use of boronated shields. However, extensive redesign efforts are indicated for the outer radial shield, the wraparound shield, and the lower axial shield configurations. These new designs have already been initiated by GA and will undergo analyses similar to those described above.

REFERENCE

1. C. O. Slater and M. B. Emmett, "Analysis of a Fuel-Pin Neutron-Streaming Experiment to Test Methods for Calculating Neutron Damage to the GCFR Grid Plate," this Conference.